

NOV 6 1991

**Evaluation of Surface Analysis Methods for  
Characterization of Trace Metal Surface Contaminants  
Found in Silicon IC Manufacturing**

**Alain C. Diebold, P. Maillot, M. Gordon, J. Baylis  
J. Chacon, R. Witowski  
SEMATECH, 2706 Montopolis Drive Austin, TX 78741**

**H. Arlinghaus  
Atom Sciences  
114 Ridgeway Center  
Oak Ridge, TN 37830**

**J. A. Knapp and B. L. Doyle,  
Sandia National Laboratory  
Albuquerque, NM 87185-5800**

**DISCLAIMER**

This report was prepared as an account of work sponsored by an agency of the United States Government. Neither the United States Government nor any agency thereof, nor any of their employees, makes any warranty, express or implied, or assumes any legal liability or responsibility for the accuracy, completeness, or usefulness of any information, apparatus, product, or process disclosed, or represents that its use would not infringe privately owned rights. Reference herein to any specific commercial product, process, or service by trade name, trademark, manufacturer, or otherwise does not necessarily constitute or imply its endorsement, recommendation, or favoring by the United States Government or any agency thereof. The views and opinions of authors expressed herein do not necessarily state or reflect those of the United States Government or any agency thereof.

**MASTER**



A major topic at recent silicon-based integrated circuit (IC) manufacturing symposia is the pursuit of decreased contamination levels. The aim is to remove contamination from both processes and materials. In conjunction with this effort, characterization methods are being pushed to lower and lower detection limits. In this paper, we evaluate surface analysis methods used to determine the concentration of inorganic contamination on unpatterned Si wafers. We compare sampling depths, detection limits, and applicability of each method for use in support of Si IC manufacturing. This comparison is further limited to Fe and Cu which are transition metal contaminants associated with manufacturing yield loss.

The surface analysis methods included in this evaluation are: Total Reflection X-Ray Fluorescence (TXRF or TRXRF); Secondary Ion Mass Spectrometry (SIMS); two "post-ionization" methods Surface Analysis by Laser Ionization (SALI) and Sputter Initiated Resonant Ionization Spectroscopy (SIRIS); Heavy Ion Backscattering Spectroscopy (HIBS); and Vapor Phase Decomposition (VPD) based methods Atomic Absorption (VPD-AA) along with VPD-TXRF. Sets of 6" Si wafers with concentration levels between  $10^9$  atoms/cm<sup>2</sup> and  $10^{12}$  atoms/cm<sup>2</sup> Fe and Cu were characterized by TXRF, SIMS, SIRIS, and HIBS. This data allows estimation of detection limits (DLs) and relative method accuracy.

In Section 1 we describe each surface analysis method and the circumstance under which it would be used to support Si IC manufacturing. The equipment used for this comparison and the 150 mm Si wafer set are described in Section 2. Results from each method are contrasted in Section 3. Finally, a conclusion is presented in Section 4.

## Section 1: TECHNIQUE DESCRIPTION

### TXRF

TXRF has become a popular method of screening Si wafers surface contamination before manufacture.[1] TXRF also provides an important means of evaluating wafer cleaning equipment and methods. This technique's success results from its ability to provide quantitative data for a wide range of elements from Na to U in a short period of time. Present generation TXRF systems are compatible with a "class 100" particle free IC manufacturing environment, and wafers are analyzed in a class 10 environment. Preliminary particle count data indicates that TXRF analyzed Si wafers can continue in the IC Manufacturing process flow.

The elemental content of inorganic contamination is observed by x-ray fluorescence excited by a grazing incidence x-ray beam. A shallow angle of incidence is selected in the range of total reflection below the critical angle,  $\theta_c$ . [1]  
 $\theta_c$  for Si = 6.1 mins of arc and  $\theta_c$  for SiO<sub>2</sub> = 5.9 mins of arc. The penetration depth  $Z_p$  of the x-ray beam for an ideal surface can be calculated using EQ2 of reference 1 where  $I/I_0 = 1/e$  for an incident x-ray intensity of  $I_0$ . [2]

$$Z_p = \frac{\lambda}{4\pi\sqrt{\delta} [ ((X^2-1)^2 + Y^2)^{1/2} - (X^2-1) ]^{1/2}}$$

Here  $\lambda$  is the wavelength of x-ray beam;  $\delta$  is the real part of refractive index;  $X = \theta / \theta_c$  incident/ $\theta_c$  critical; and  $Y = \beta / \delta$  where  $\beta$  is the imaginary part of the refractive index. One can use  $\theta_c$  [SiO<sub>2</sub>] since  $\theta_c$  does not drastically change as the x-ray beam crosses the native oxide to reach the Si. For  $\theta = 1.3$  mrad, the penetration depth  $Z_p = 50$  Å for Mo, Cu, and W(K) radiation.

The true penetration depth is considerably greater due to surface roughness, wafer warpage, and beam divergence. Careful TXRF measurements require use of a wafer chuck that corrects wafer warpage. Work at Texas Instruments has estimated  $Z_p$  using buried CaF<sub>2</sub> layers.[3] A penetration depth of greater than 100 nm has been reported by Dr. Hossain and other workers.[3] Due to the difference between TXRF instrument designs, penetration depth depends on x-ray beam divergence. Therefore, comparison of sputter profile data and TXRF requires integrating concentration to at least 15 nm. Common sense indicates that since the major contribution to total concentration typically comes from the top 10 to 15 nm, integrating to greater depth may not be necessary. The next question is how to weight the contributions vs depth.

Since the analysis depth of each method differs, the penetration depth  $Z_p$  for TXRF is a critical aspect of technical comparison. The near atomic layer by atomic layer concentration information from sputter initiated methods such as SALI and SIRIS must be integrated over the TXRF sampling depth. VPD sampling depth depends on the native oxide thickness and chemical interactions between contaminant and Si wafer surface.

Quantification of TXRF relies on daily calibration of instrument response. Typically the standard is a nanogram of Ni located in a small area at the center of the wafer. The analysis area (~8mm) must cover the wafer area containing the Ni. Atomic adsorption spectroscopy standard solutions are well characterized and easily diluted to make the nanogram Ni standard. Using fluorescence yield curves, software can calculate the instrument response for other elements. A more rigorous approach is to calibrate the fluorescent yield for each element of interest. Unfortunately this would require approximately 10 to 20 minutes per element. A more productive strategy is to sample multiple areas of each wafer for contamination uniformity.

TXRF is also capable of determining the nature of the inorganic contamination. [1] Particulate or residue does not participate in total reflection. Its fluorescent intensity remains roughly constant as the angle of incidence of the x-ray beam is increased to the critical angle, and it decreases by roughly 1/2 for angles greater than  $\theta_c$ . Contamination that is plated or more uniformly distributed in the native oxide does participate in total reflection. Both of these responses are shown in figure 1, and are called angle plots. Here,

the fluorescent intensity rapidly increases as one approaches the critical angle and decreases when  $\theta > \theta_c$ . In figure 2, we show the result obtained for angle plots of the two types of contaminated wafer surfaces analyzed in this study. The reason for the selection of  $1.3 \mu$  rad for the angle of incidence of Mo x-ray beams is now more apparent. The fluorescent intensity of equal amounts of residue and plated contamination should be nearly equivalent. This allows one to use the residue like Ni STD to calibrate the TXRF for plated samples.

A summary of the above information is required for subsequent discussion. Several approximations have been used in quantifying TXRF. First, one assumes that the response of residue and plated samples is identical for the selected angle of incidence. Second, the TXRF instrumental response closely matches fluorescent yield curves. Finally, the precision of the measurement must be considered for each level of contamination from  $10^{12}$  atoms/cm<sup>2</sup> to  $10^9$  atoms/cm<sup>2</sup>. Typical reproducibilities for new generation TXRF units equipped with a rotating anode source for Fe and Cu are 2% standard deviation for concentrations in the low  $10^{11}$  atoms/cm<sup>2</sup> range.

## SIMS

Secondary ion mass spectrometry is an excellent method of determining both bulk dopant concentrations and surface composition. In this method, a beam of primary ions ( $\text{Ar}^+$ ,  $\text{Cs}^+$  or  $\text{O}_2^+$ ) sputters the sample surface. A small fraction of the ejected particles are ions which are analyzed by mass spectrometry. It is well known that surface information can be obtained by using static SIMS. Static SIMS conditions occur when part of a monolayer of the surface atoms are sputtered during the analysis. In Quasi Static SIMS, one samples only a few atomic layers at a time. When used in the static mode, SIMS provides non-quantitative information about surface elemental contamination. For example, Al is not observed in TXRF, while it is readily observed by SIMS. We do not discuss the use of poly-encapsulated SIMS. This method requires processing equipment not generally available in a laboratory setting.[ ] After discussion of post-ionization methods, we compare calculated detection limits for all sputter initiated methods.

"Post-ionization" analysis techniques allow quantification of surface elemental composition.[4] The sputtered neutrals are ionized by either non-resonant ionization in SALI or by resonant ionization in SIRIS (or SARISA) before mass analysis. The advantage of these methods lies in the lower ultimate detection limits and the ability to analyze large areas of patterned wafer samples.

## SALI

SALI [Surface Analysis by Laser Ionization] is the acronym used for non-resonant laser ionization of sputtered neutral species.[5] In SALI, both the neutral and excited atomic and multimer (ie.,  $\text{Si}_2$ ) are ionized using UV radiation from KrF excimer laser and then mass analyzed.[5] Thus the mass spectrometer must distinguish between isobaric particles such as Fe and  $\text{Si}_2$  ( $M/M = 10,000$ ). Although Time of Flight (TOF) mass analyzers are known to have mass resolutions approaching 10,000, the interplay between the nano second long laser pulse and the 0.5 to 1 microsecond long ion pulse results in

much lower SALI mass resolution.[4] Young et al. indicate that SALI mass resolution of 500 has been achieved using a reflectron while SARISA is capable of 200 mass resolution. One critical but often neglected aspect of SALI is the effect of changes in ionizing laser intensity on the volume of analyzed sputtered particles.[5] Saturation of the ionization requires very high laser power in the range of  $10^{11}$  watts/cm<sup>2</sup>. The laser must be focused into an area of  $10^{-3}$  cm<sup>2</sup>. The effect of laser stability and system optics on analysis volume makes quantitative measurement difficult. Since homogeneously surface doped standard wafers do not exist, accessing the reproducibility of SALI for this application is difficult.

The increased complexity of SALI over TXRF must result in lower detection limits and quantitative analysis. One recent study has shown detection limits down to low  $10^{10}$  atoms/cm<sup>2</sup> for Fe on Si.[6]

### SARISA/SIRIS

The use of resonant ionization to analyze sputtered particles goes by two acronyms: SARISA and SIRIS. Both terms have been used to distinguish the unique instrument design used by the group naming this technique. A review of these methods is currently in progress. The atom of choice is selectively analyzed by post-ionization of sputter initiated particles followed by mass spectrometric detection. Under very controlled conditions, SIRIS can detect much less than  $1 \times 10^5$  atoms/cm<sup>2</sup>. This proof of concept was done at Pennsylvania State University by Winograd et al.[7] and at Atom Sciences using a set of well characterized In doped Si wafers.[8] The sample surface was prepared in-situ by ion etching the surface until a stable response was observed. Furthermore, practical analysis requires a much higher throughput than that used for these measurements.[4,9] In this work, we approach the question of detection limits under conditions that might apply for industrial analysis laboratories.

In SARISA/SIRIS, either two or three wavelengths of light are focused into an area  $\sim 10^{-2}$  cm<sup>2</sup> with an intensity less than  $10^6$  watts/cm<sup>2</sup>. [4,6] Saturation of the ionizing transition requires approximately one order of magnitude more intensity. Since resonant transitions are used, the various atomic transitions saturate at a much lower intensity than the completely non-resonant SALI ionization. The importance of correct selection of the ionization scheme lies in the ability to remove interference from non-resonant processes. Again, one must correct [or remove] the contribution of non-resonantly ionized Si<sub>2</sub><sup>+</sup> to the Fe<sup>+</sup> signal.[4,9] The Si<sub>2</sub><sup>+</sup> signal will vary with matrix. For example, one expects minimal Si<sub>2</sub><sup>+</sup> from SiO<sub>2</sub> and considerable Si<sub>2</sub><sup>+</sup> from Si. The ionization schemes used in this work are listed in Table 2.

### COMPARISON OF DETECTION LIMITS FOR SPUTTER INDUCED METHODS

It is interesting to compare the detection limits of sputter initiated methods. In this paper, the detection limit for atomic fraction is calculated as follows:

$$N = n_p \times S \times C \times \delta$$

*N = the number of counts detected:  $n_p$  is the total primary ion dose sputtering the surface. For a pulse source,  $n_p$  equals the number of primary ions / pulse  $\times$  the number of pulses. S is the sputter rate, here  $S = 2$ . C is the atomic fraction of the contaminant.  $\delta$  is the useful yield = ions detected / atoms sputtered.*

In SIMS, the useful yield is a product of the secondary ion yield, the fraction of ions that enter the ion optics, and the mass spectrometer transmission,  $\Psi_m$ . We assume a useful yield of  $\delta = 10^{-4}$  for Fe.

Young, et al, [4] present an excellent discussion of the factors governing the ultimate detection limit for post-ionization methods. Our calculated detection limits for sputter initiated methods are based on this work. Increasing detection limits requires a design that optimizes three factors. First, the number of neutral atoms entering the laser ionization region must be maximized. Second, the overlap between the area of ionizing light and the sputtered particle cloud must be optimized. As mentioned below, the effective region of interaction between laser light and sputtered atoms is smaller in SALI. Finally, the transmission of the extraction lens-mass spectrometer should be close to unity. The useful yield,  $\delta$ , is a product of the fraction of sputtered atoms that are photoionized  $\Psi_a$  times the mass spectrometer transmission factor  $\Psi_m$ . [4]

In order to calculate a detection limit for SALI, a value for the useful yield must be estimated. Young et al estimate  $\Psi_a$  to be 0.01 to 0.03 for SALI. Becker [5] proposes that  $\delta = 0.001$  while Young suggest  $\delta = 0.01$  [4] as obtainable for most sputtered atoms. Our calculated detection limit for SALI agrees with the  $1 \times 10^8$  limit proposed by Becker.

In both SARISA and SIRIS, one expects a much higher useful yield than for SALI. Since the laser volume resulting in ionization is larger,  $\Psi_a$  values from 0.05 to 0.15 are possible according to Young. [4] The reported mass spectrometer transmission factor for SARISA is unity thus giving the SARISA apparatus an advantage in ultimate detection limits. The useful yield for SARISA is typically  $\delta = 0.1$ , and  $\delta = 0.05$  was reported for detection of Fe implanted in silicon. [9] We estimate the useful yield of SIRIS for iron as  $\delta = 0.005$  from a calibration of 1 count per 1000 shots for 10ppb Fe [1 count per shot for 7.5 ppb Cu results in  $\delta = 0.007$  for Cu].

The calculated detection limits are listed in Table 2. These estimates show that resonant post-ionization techniques should have a distinct advantage over other sputter initiated methods when they are applied to trace analysis of inorganic contaminants. Below, we compare SIRIS with other non-sputter initiated methods.

## HIBS

Heavy Ion Backscattering Spectrometry (HIBS),<sup>10,11</sup> is a new ion beam analysis technique that uses the backscattering of moderate energy (a few hundred KeV) heavy ions. A sensitivity for medium-to-heavy surface impurities of ~1000x greater than conventional Rutherford Backscattering Spectrometry (RBS) has been demonstrated, and improvements with further developments are anticipated. RBS is typically performed using a 1-2 MeV He<sup>+</sup> ion beam for the analysis resulting in a sensitivity of ~10<sup>13</sup> atoms/cm<sup>2</sup> to impurities at or near the surface. RBS sensitivity is limited by system noise. Backscattering yield is proportional to the square of the atomic number (Z<sup>2</sup>) of the analyzing beam and inversely proportional to the square of its energy. Therefore, an enhanced yield can be obtained by using a higher Z ion beam at lower energy. Although this yield enhancement is well known, it has not been previously exploited because detector signal pileup due to yield from the lower mass substrate overwhelms the signal from ions scattered by trace surface impurities. This problem was eliminated by introducing a thin, self supporting C foil in front of the detector to range out particles scattered from the substrate. The thickness of this C foil is chosen such that ions scattered from impurities lighter than silicon lose all of their energy and thus never reach the detector, while ions scattered from impurities heavier than the substrate (which have a higher energy) make it through the foil and are counted. Using a 200 - 400 KeV C<sup>+</sup> beams (other ions such as B<sup>+</sup> or N<sup>+</sup> would serve as well) and solid-state surface barrier detectors, sensitivities as high as 8x10<sup>8</sup> atoms/cm<sup>2</sup> for Au on a silicon substrate have been demonstrated. A significant advantage of the technique is that HIBS can detect all elements heavier than Ar with a sensitivity proportional to Z<sup>2</sup>.

## VPD

VPD is a method of removing the native oxide layer from the wafer surface for trace metal analysis.[12] Usually Atomic adsorption spectroscopy (AA) and TXRF are used to analyze the resulting solution. VPD chambers contain acid resistant beakers and wafer holders. The beaker containing the etchant solution is warmed allowing HF in the chamber ambient. Typically, VPD of the native oxide surface is accomplished by reaction of HF with SiO<sub>2</sub> forming H<sub>2</sub>SiF<sub>6</sub> and H<sub>2</sub>O. The metal contaminants are concentrated in a droplet [50 microliters] of water that is rolled across the wafer surface. The water droplet is dried on a Si wafer surface for VPD-TXRF or collected for VPD-AA.

Meuris et al. report using 0.5%HF/1%H<sub>2</sub>O<sub>2</sub>/98.5%H<sub>2</sub>O to remove the native oxide layer. They report the collection efficiency for Fe as being roughly 80% and 15 to 20% for Cu with an collection accuracy of 10% for most metals in the 5 x 10<sup>11</sup> range. The collection error in the 1 x 10<sup>9</sup> atoms/cm<sup>2</sup> range is a factor of from 2 to 5. Cu collection accuracy is reported to be much less favorable. These initial studies indicate that VPD is capable of measuring in the 1x 10<sup>9</sup> atoms/cm<sup>2</sup> range. Further study of VPD is required. For example, the effect of chemical state on collection efficiency and VPD sampling memory effects are unknown. Usually, the AA or TXRF measurement error is small compared to error due to VPD collection.

## Section 2: Experimental

A set of 150mm Si wafers were used to compare characterization methods. One of the wafers was a commercial epitaxial silicon covered Si substrate. Some of the wafers were dosed with Fe and Cu by ashing a photoresist coated surface using commercial IC processing equipment. Dosing changes were accomplished by varying the photoresist thickness. The photoresist used in this study left relatively uniform Fe and Cu contaminations levels. Other wafers were prepared by cleaning photoresist coated samples. Cleaning processes could be altered to selectively leave a majority of the Cu dose on the surface. Other wafer surfaces were prepared using standard solutions of Fe or Cu.

The mobility and diffusivity of Fe and Cu must be accounted for if this comparison is to be meaningful. Since the samples were not heat treated, these effects should be minimized. One interesting test of this process is the comparison of TXRF analysis at two different locations, SEMATECH and Charles Evans Associates.

TXRF analysis was done using both the Perkin Elmer/Atomika XSA 8000 and a new generation TXRF that employs a rotating anode. The new generation TXRF data was taken at Charles Evans Associates by Dick Hockett. The Atomika TXRF response was calibrated using a Ni dosed wafer surface at  $20.413 \times 10^{12}$  atoms/cm<sup>2</sup> and the Charles Evans data was calibrated using a Cu dosed Si wafer at  $23.0 \times 10^{12}$  atoms/cm<sup>2</sup>. Both standards are checked by Rutherford Backscattering Spectroscopy. It is important to note that Hockett has observed a factor of 1.5 more Cu when samples are measured using the Atomika vs the new generation TXRF.

The SIRIS data was taken at Atom Sciences using specially designed equipment. Additional resonant ionization data was obtained from the SARISA apparatus by W. Calaway. The SIRIS data was quantified by integrating the signal over the 1st 15nm of the depth profile. Sensitivity factors were obtained from TXRF data for samples having approximately  $3\text{-}5 \times 10^{12}$  atoms/cm<sup>2</sup> of Fe or Cu. The inability to distinguish Fe from Cu prevented the use of HIBS data for calibration purposes. The background signal observed in epitaxial silicon was 100ppb for Fe and Cu. This represents the instrumental background signal since epitaxial silicon is known to have only ppt levels of these metals.

The HIBS data shown here were obtained with a 250 KeV C<sup>+</sup> beam and a single surface barrier detector (0.1 sr solid angle). The beam spot was 2mm in diameter and a total of 50 microC of charge was used for each analysis. Because of the limits in energy resolution for surface barrier detectors, the peaks due to Fe and Cu cannot be easily deconvoluted. For samples with both elements, only the total of the two can be measured, although analysis of the peak shape gives an approximate ratio between the two elements. In each case, this ratio was consistent with the results from TXRF.

One notable aspect of this study is the lack of standards for calibration of instrument response at concentration levels of  $1 \times 10^{12}$  and below. The standard of choice depends on your geographical location. In the U.S., RBS is usually considered the method of choice for verification of standard samples for TXRF. Due to the reported variability of VPD at low

concentration levels, it is not an acceptable standardization method. Other methods include, as mentioned in the description of TXRF in section 1, dosing a known amount of metal in the analysis area of TXRF.

### Section 3: EXPERIMENTAL RESULTS

Typical results for HIBS and SIRIS are shown in figures 3,4, and 5. TXRF spectra show excellent signal to noise for concentrations of Fe and Cu close to  $1 \times 10^{10}$  atoms/cm<sup>2</sup>. SIRIS depth profile data for several different levels of Fe and Cu are shown in separate figures. **As mentioned above the HIBS data are for the total Fe and Cu since these metals cannot be resolved using a surface barrier detector.**

TOF-SIMS data was obtained for a sample containing Fe at a low  $10^{10}$  atoms/cm<sup>2</sup> level. The TOF spectra clearly separated the Fe and Si<sup>2</sup> dimer peaks. This indicates that TOF-SIMS can be used to observe metal contamination, and that the detection limit may be  $< 1 \times 10^{10}$  atoms/cm<sup>2</sup>. Since this mode of SIMS analysis is not quantitative, a complete sample set was not analyzed.

In Table 3, the results of analysis of identical wafer samples are listed. All analysis methods show the same trends in measured concentration levels. Both TXRF and SIRIS show the ability to measure concentrations of Cu below  $1 \times 10^{10}$  atoms/cm<sup>2</sup>, and SIRIS responses can be attributed to concentrations below  $5 \times 10^9$  atoms/cm<sup>2</sup>. An estimate of the detection limit for Fe by SARISA can be obtained from published data for Fe implanted silicon wafers. This indicates a Fe DL of roughly  $5 \times 10^8$  atoms/cm<sup>2</sup> for SARISA and thus "state of the art" resonant "post-ionization" methods.

The SIRIS depth profile data for Fe indicate that the instrument has a very high background problem limiting detection limits well above the  $1 \times 10^8$  atoms/cm<sup>2</sup> calculated detection limit. Since the primary ion beam is not mass filtered, both Fe and Cu can come from the probe beam itself. For this reason, Fe concentrations are not reported in table 3 for part of sample set 2. We are investigating the source of the background with Gruen, Pellin, Callaway, and Young at Argonne National Laboratory through SARISA analysis.

All the methods show the same trend in concentration vs sample. One aspect of this study is that the need for standards is pointed out. HIBS could be used to standardize samples when contaminant mobility and diffusivity are accounted for. There is good agreement between TXRF measurements considering that two different TXRF systems were used and that system calibration is different. This indicates that the general trends observed in this study are valid.

The detection limits that this study addresses require class 100 or better sample introduction. Future analysis will require the class 10 areas already used for TXRF. This places some uncertainty in a technique comparison. Although great care was taken in sample preparation, sample handling contamination could explain some of the differences seen in the data for the "undosed clean A" wafer in sample set 2. We plan on continuing

this study.

#### Section 4: CONCLUSIONS

In Table 4, we summarize a comparison of the techniques discussed in the paper. Clearly, method selection is based on the importance one places on factors such as analysis time and the destructive nature of the sample. HIBS stands out from the other methods in its ability to provide quantitative data with the use of standards. The low cost of VPD and TXRF's ability to do non-destructive analysis have made both of these methods very popular for support of IC manufacture. Both the "post-ionization" methods and HIBS have a much broader range of applicability for materials characterization than the other methods.

without

The final conclusion of this study is that this type of method comparison should continue. It allows one the opportunity to identify all the issues tied to each analysis technique, and it should foster the cooperative spirit needed for further development.

#### ACKNOWLEDGEMENTS

We gratefully acknowledge discussions of "post-ionization" methods with Dieter Gruen, Michael Pellin, Charles Young, and Wally Calaway of Argonne National Laboratory. We also acknowledge input from Chris Becker on the ultimate detection limits of SALL. Continuing discussion with Mark Anthony, Joe Keenan, and Tim Hossain of Texas Instruments have contributed greatly to our knowledge of all these methods. We also thank Ara Philipossian of Digital Equipment and Kim Gupta of Intel for increasing our understanding of VPD.

TABLE 1

## Resonant Ionization Schemes

| Fe   | Cu   |
|--|--|
| $a^5D_4$ to $y^5F^{\circ}_5$ 296.69nm [12uJ] | $4s^2S_{1/2}$ to $4p^2P^{\circ}_{3/2}$ 324.75nm [15uJ] |
| $y^5F^{\circ}_5$ to continuum 323.8nm [10uJ] | $4p^2P^{\circ}_{3/2}$ to $6d^2D_{5/2}$ 368.74nm [5uJ]  |
|  | $6d^2D_{5/2}$ to continuum 7064nm [2-3uJ]              |

TABLE 2  
CALCULATED DETECTION LIMITS FOR  
SPUTTER INDUCED POST-IONIZATION TECHNIQUES

C is calculated using  $1 \times 10^{10}$  primary ion dose unless stated otherwise.

$$N = n_p \times s \times C \times \delta$$

$n_p$  = number of primary ions/pulse  $\times$  number of pulses  
 $\delta$  = useful yield  
 $s$  = sputter yield  
 $C$  = atomic fraction  
 Assume  $N = 10$  counts

(3)

| METHOD                           | PRIMARY ION CONDITIONS   | USEFUL YIELD  | C DL IN ATOMIC FRACTION  | DL FOR Fe in Si ATOMS/CM <sup>2</sup> |
|----------------------------------|--|---------------|--|---------------------------------------|
| SIRIS<br>ATOM SCIENCES<br>[8]    | 9 KeV 1.55uA<br>0.00018cm <sup>2</sup> spot<br>500ns<br>3000 pulses                                      | 0.005         | $7 \times 10^{-8}$   | $1 \times 10^8$                       |
| SARISA<br>ARGONNE NL [4]         | 1-5 KeV 2uA<br>0.00018cm <sup>2</sup> spot<br>500ns 3000 pulses<br><br>$1.8 \times 10^5$ pulses          | 0.05          | $1 \times 10^{-8}$<br><br>$1 \times 10^{-10}$                        | $1 \times 10^7$                       |
| EARNs<br>WINOGRAD PENN STATE [7] | 10 KeV $46 \mu A$<br>0.071cm <sup>2</sup> spot<br>5600ns<br>9000pulses 30Hz<br>dose $1.3 \times 10^{13}$ | 0.05?<br>0.1? | $8 \times 10^{-12}$<br>$4 \times 10^{-12}$<br>$1 \times 10^{-12}$ In | $1 \times 10^4$                       |
| SALI<br>BECKER<br>SRI            |  | 0.001         | $5 \times 10^{-7}$   | $7 \times 10^8$                       |
| TOF-SIMS                         |  | 0.0001        | $1 \times 10^{-6}$   | $1 \times 10^9$                       |

TABLE 3  
 COMPARISON OF HIBS, SIRIS, and TXRF  
 Fe [Cu] CONCENTRATION in  $10^{10}$  ATOMS/CM<sup>2</sup>

| SAMPLE DESCRIPTION    | ATOMIKA TXRF  | NEW TXRF  | SIRIS                          | HIBS Fe + Cu |
|-----------------------|---------------|-----------|--------------------------------|--------------|
| SAMPLE SET 1          |               |           |                                |              |
| VIRGIN WAFER          | <DL [ $<DL$ ] |           | 56 [0.7]                       | <DL          |
| EPI-Silicon           | <DL [ $<DL$ ] |           | 3.6 [0.4]                      |              |
| RESIST DOSED WAFER #1 | 230 [120]     | 500 [150] | 230 [120]<br>SIRIS CALIBRATION | 310          |
| RESIST DOSED WAFER #2 | 130 [90]      |           | 160 [28]                       |              |
| Fe/Hcl DOSED WAFER    | 500 [ $<DL$ ] |           | 840 [5.9]                      | 350          |
| RD#1 CLEAN A          | <DL [80]      | 6 [85]    | 28 [18]                        | 28           |
| RD#1 CLEAN B          | <DL [ $<DL$ ] | 7.5 [9.5] | 5.6 [7.1]                      |              |
|                       |               |           |                                |              |

| SAMPLE DESCRIPTION    | ATOMIKA TXRF  | NEW TXRF      | SIRIS     | HIBS Fe + Cu |
|-----------------------|---------------|---------------|-----------|--------------|
| SAMPLE SET 2          |               |               |           |              |
| EPI-SILICON           | <DL [ $<DL$ ] | <DL [ $<DL$ ] | <DL [2]   | <20 ie, <DL  |
| RESIST DOSED WAFER #1 |               | 80 [45]       | STD [STD] | 90 - 190     |
| UNDOSED CLEAN A       | <DL [ $<DL$ ] | 15 [6]        | [10]      | 50 - 90      |
| RESIST DOSED CLEAN B  |               | 55 [12]       | [22]      | 70 - 100     |
| RESIST DOSED CLEAN B  | <DL [ $<DL$ ] | <DL [20]      | [40]      | <40          |
| Fe/Hcl DOSED WAFER    | [--]          | 400 [--]      | 200 [20]  | 100 - 190    |

TABLE 4  
COMPARISON OF ANALYTICAL METHODS USED TO  
CHARACTERIZE TRACE CONTAMINATION

| CAPABILITY                                  | TXRF                 | HIBS                    | SIRIS  | VPD/AA<br>VPD/TXRF   | TOF-SIMS             |
|---|----------------------|-------------------------|--|--|----------------------|
| Fe AND Cu<br>DETECTION<br>LIMIT             | $< 1 \times 10^{10}$ | $\sim 1 \times 10^{10}$ | $\sim 1 \times 10^{10}$ Fe<br>$< 1 \times 10^{10}$<br>Cu | $\sim 1 \times 10^9$<br>TXRF<br>$\sim 1 \times 10^8$<br>AA | $< 1 \times 10^{10}$ |
| PREDICTED<br>FUTURE DL                      | $1 \times 10^9$      | $\sim 5 \times 10^9$    | $\sim 1 \times 10^9$ Fe<br>$\sim 1 \times 10^8$ Cu       | $\sim 1 \times 10^8$<br>TXRF<br>??                         | $1 \times 10^9$      |
| REQUIRES<br>STANDARD                        | YES                  | NO                      | YES  | YES *  |                      |
| QUANTITATIVE                                | YES                  | YES                     | YES  | 2-5X<br>ERROR<br>$< 1 \times 10^{10}$                      | NO                   |
| DESTRUCTIVE                                 | NO                   | YES                     | YES  | YES  | YES                  |
| ANALYSIS<br>TIME                            | 10 MINS              | 30 MINS                 | 10/DAY   | $< 25$ MINS  | 10 MINS              |
| WAFER<br>CASSETTE<br>AUTOMATED              | YES                  | NO                      | NO   | NO   | NO                   |
| AVAILABILITY<br>(C)OMMERCIAL<br>(P)ROTOTYPE | C                    | P                       | P  | C  | C                    |

\* Requires collection efficiency information for each metal for etchant solution selected.

## Figure Captions

Figure 1. Plot of the intensity of x-ray fluorescence vs angle of incidence of the x-ray beam for the silicon substrate, contamination present in a reflective layer, and contamination present in a non-reflective or particulate type layer.

Figure 2. Plot of Fe and Cu contamination x-ray fluorescent intensity vs angle of incidence of the x-ray beam for a layer of photoresist that was removed from the surface by ashing.

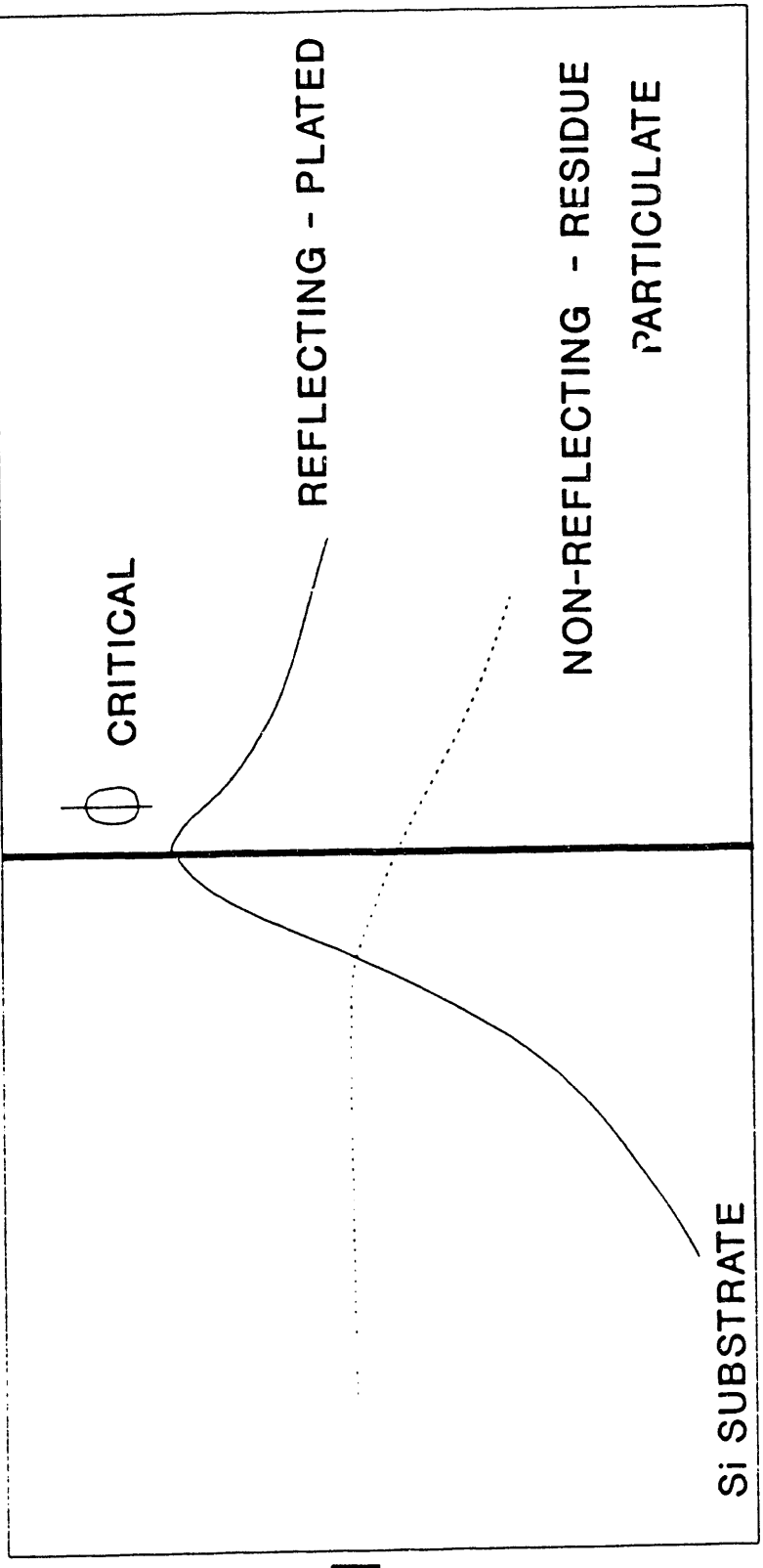
Figure 3. Plot of a HIBS spectra for a contaminated surface.

Figure 4. SIRIS depth profile data for Fe contaminated surfaces and an epitaxial silicon surface. To allow technique comparison, the Fe concentrations were taken from TXRF data.

Figure 5. SIRIS depth profile data for Cu contaminated surfaces and an epitaxial silicon surface. The Cu concentrations were taken from TXRF data.

## REFERENCES

1. H. Schwenke, W. Berneike, J. Knoth, and U. Weisbrod, Advances in X-Ray Analysis, **32**, C. Barrett and J. Gilfrich, R. Jenkins, T. Huang, eds, p 105, Plenum, (1989).
2. L. G. Parrat, *Phys. Rev.* **95**, 359 (1954).
3. T. Housain, J. Keenan, and J. M. Anthony, private communication.
4. C.E. Young, M.J. Pellin, W.F. Calaway, B. Jorgensen, E.L. Schweitzer, and D.M. Gruen, *Nucl. Inst. Meth. in Physics Res.*, **B27**, 119 (1987).
5. C.H. Becker, S.G. McKay, and D.G. Welkie, *JVST-B*, in press.
6. S. Daiser, *IEEE Circuits and Devices*, **7**, 27 (1991).
7. D.L. Pappas, D.M. Hrubowchak, M. H. Ervin, and N. Winograd, *Science*, **243**, 64 (1989).
8. H.F. Arlinghaus, M.T. Spaar, and N. Thonnard, *JVST A*, **8**, 2318 (1990).
9. M.J. Pellin, C.E. Young, W.F. Callaway, J.E. Whitten, D.M. Gruen, J.D. Blum, I.D. Hutcheon, and G.J. Wasserburg, *Phil. Trans. R. Soc. Lond. A* **333**, 133 (1990).
10. B.L. Doyle, J.A. Knapp, and D.L. Buller, *Nucl. Inst. and Meth.* **B42**, 295 (1989).
11. J.A. Knapp and B.L. Doyle, *Nucl. Inst. and Meth.* **B45**, 143 (1990).
12. M. Meuris, M. Heyns, W. Kuper, S. Verhaverbeke, and A. Philipossian, ECS, Washington D.C. May 1991.



ANGLE OF INCIDENCE

Figure 1

TXRF ANGLE SCAN  
Fe and Cu from ashed resist

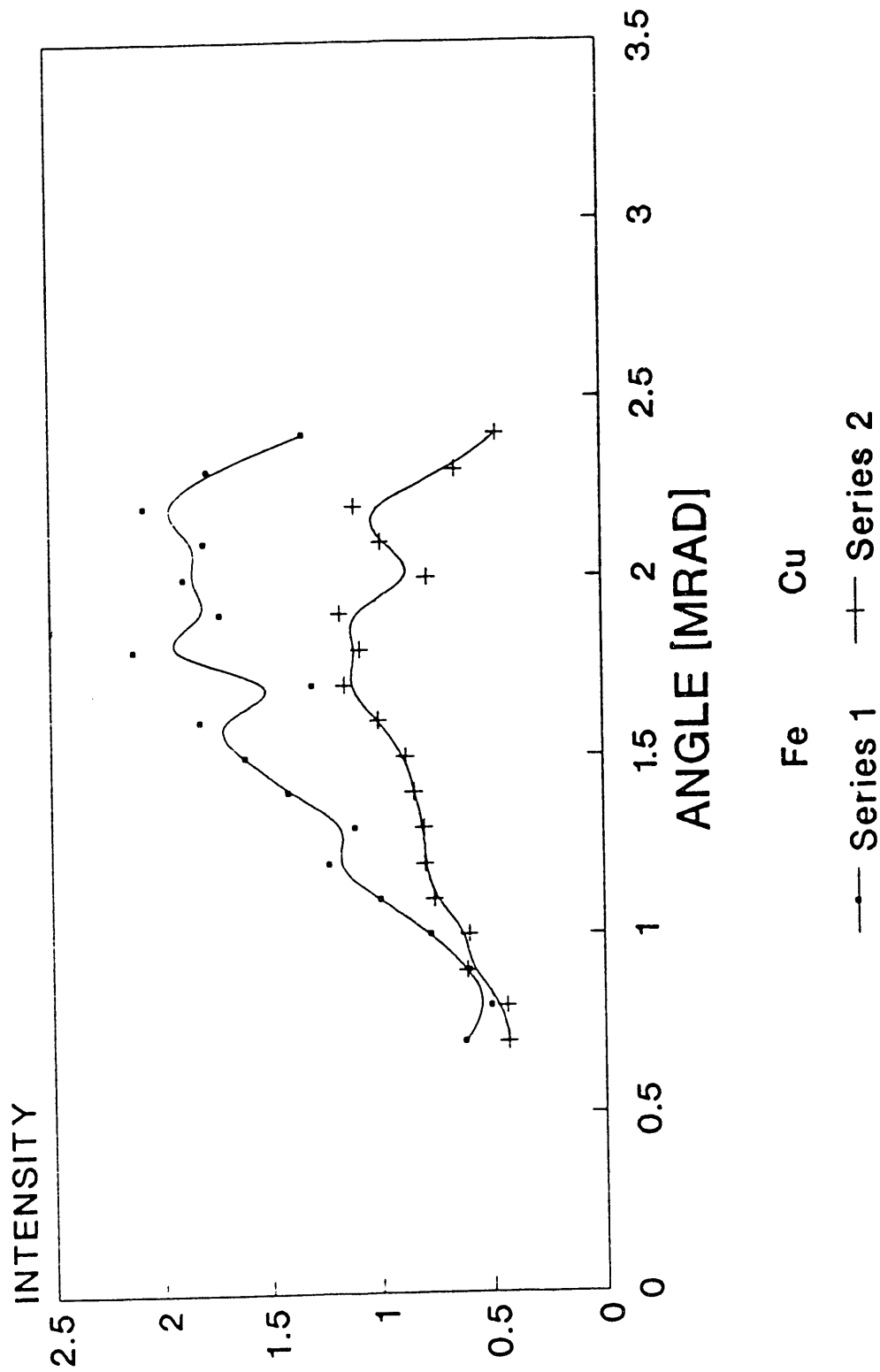


Figure 2

- (a) Fe/Cu dosed - no clean
- (b) Clean epi Si

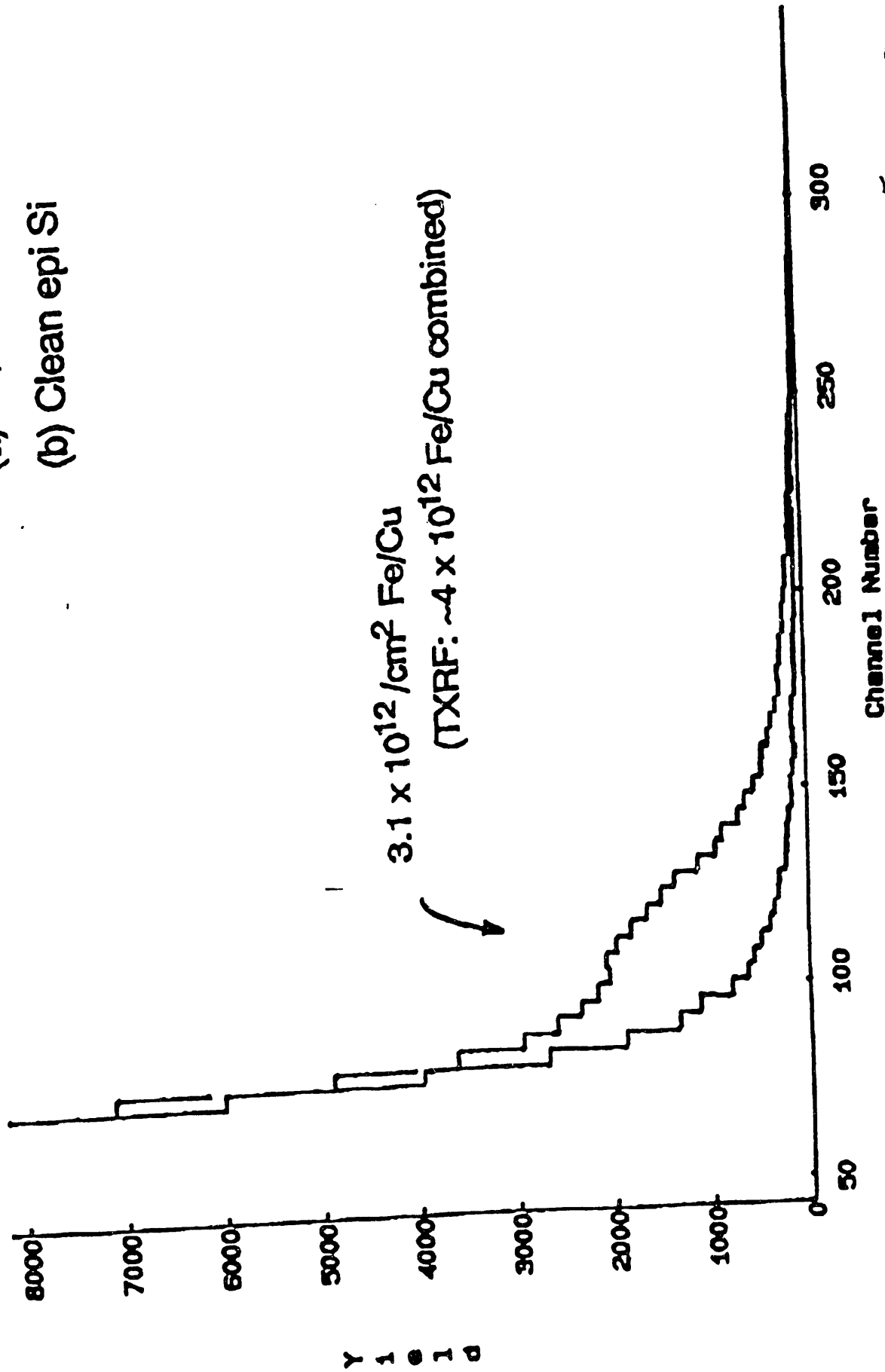


Figure 3

# SIRIS DEPTH PROFILE

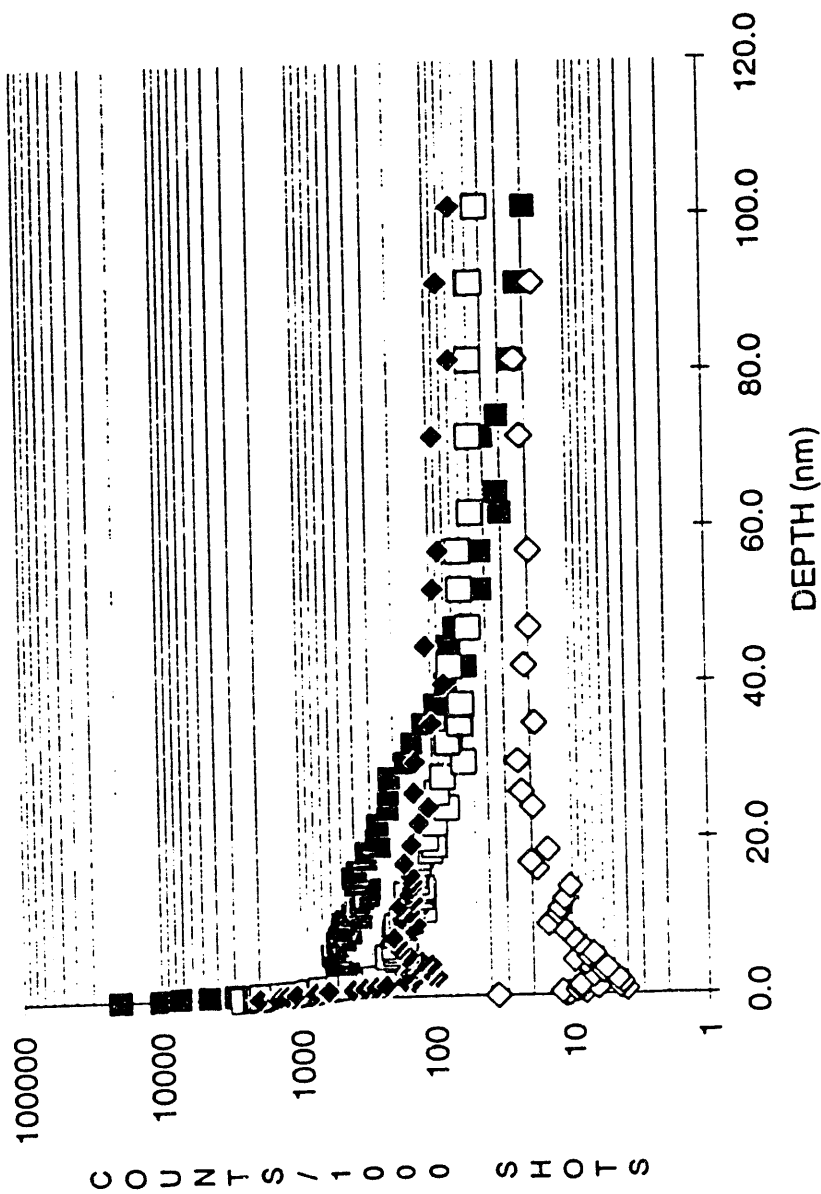


Figure 4

# SIRIS DEPTH PROFILE

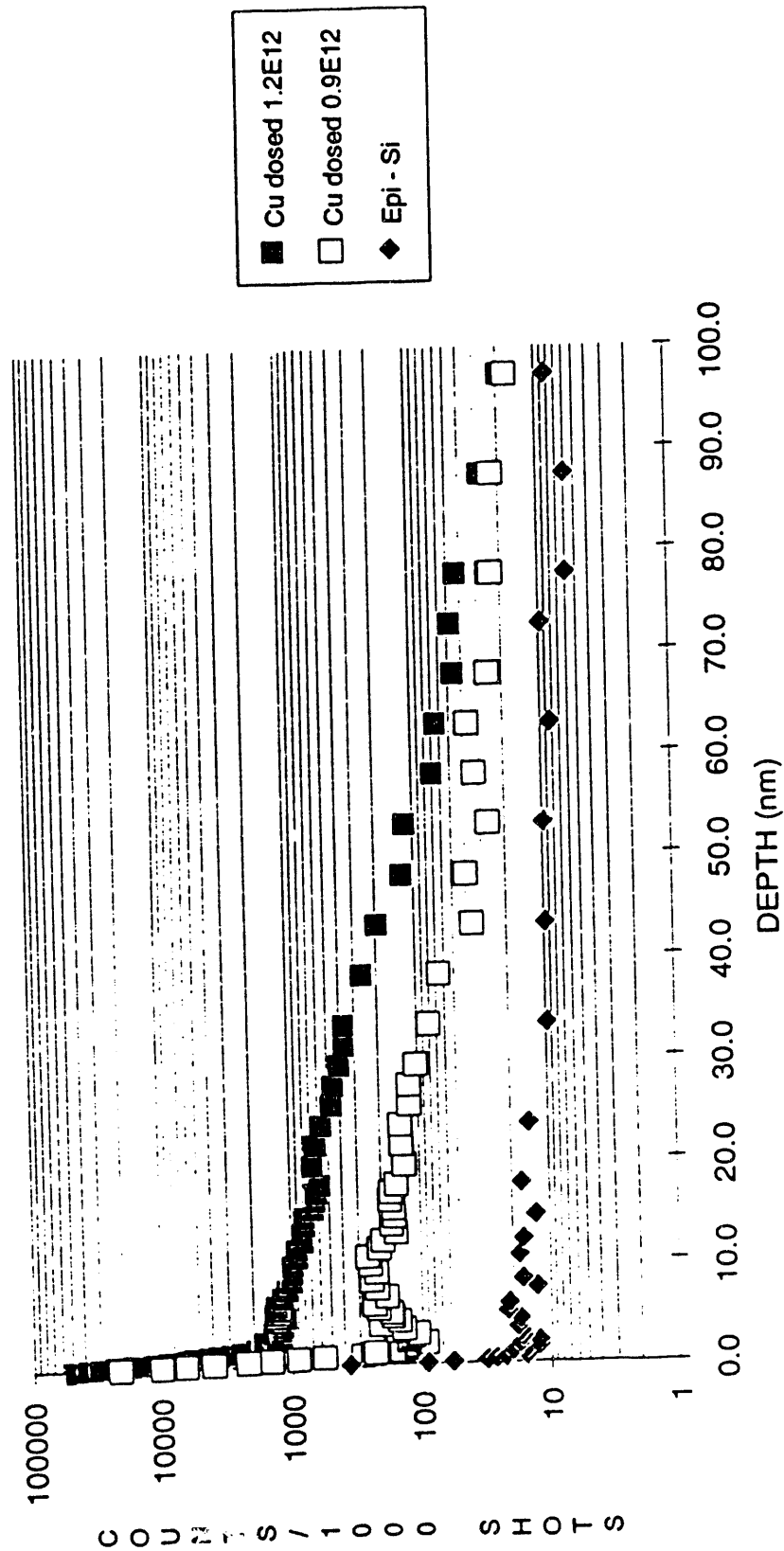


Figure 5

**END**

**DATE  
FILMED**

*12/24/91*

\_\_\_\_\_

\_\_\_\_\_